

LATE-TIME SPECTRAL OBSERVATIONS OF THE STRONGLY INTERACTING TYPE IA SUPERNOVA PTF11KX

JEFFREY M. SILVERMAN^{1,2,3}, PETER E. NUGENT^{2,4}, AVISHAY GAL-YAM⁵, MARK SULLIVAN⁶, D. ANDREW HOWELL^{7,8}, ALEXEI
V. FILIPPENKO², YEN-CHEN PAN⁹, S. BRADLEY CENKO², AND ISOBEL M. HOOK^{9,10}

Draft version October 3, 2018

ABSTRACT

PTF11kx was a Type Ia supernova (SN Ia) that showed time-variable absorption features, including saturated Ca II H&K lines that weakened and eventually went into emission. The strength of the emission component of H α gradually increased, implying that the SN was undergoing significant interaction with its circumstellar medium (CSM). These features, and many others, were blueshifted slightly and showed a P-Cygni profile, likely indicating that the CSM was directly related to, and probably previously ejected by, the progenitor system itself. These and other observations led Dilday et al. (2012) to conclude that PTF11kx came from a symbiotic nova progenitor like RS Oph. In this work we extend the spectral coverage of PTF11kx to 124–680 rest-frame days past maximum brightness. The late-time spectra of PTF11kx are dominated by H α emission (with widths of full width at half-maximum intensity ≈ 2000 km s⁻¹), strong Ca II emission features ($\sim 10,000$ km s⁻¹ wide), and a blue “quasi-continuum” due to many overlapping narrow lines of Fe II. Emission from oxygen, He I, and Balmer lines higher than H α is weak or completely absent at all epochs, leading to large observed H α /H β intensity ratios. The H α emission appears to increase in strength with time for ~ 1 yr, but it subsequently decreases significantly along with the Ca II emission. Our latest spectrum also indicates the possibility of newly formed dust in the system as evidenced by a slight decrease in the red wing of H α . During the same epochs, multiple narrow emission features from the CSM temporally vary in strength. The weakening of the H α and Ca II emission at late times is possible evidence that the SN ejecta have overtaken the majority of the CSM and agrees with models of other strongly interacting SNe Ia. The varying narrow emission features, on the other hand, may indicate that the CSM is clumpy or consists of multiple thin shells.

Subject headings: supernovae: general — supernovae: individual (PTF11kx) — stars: circumstellar matter

1. INTRODUCTION

Type Ia supernovae (SNe Ia), the result of the thermonuclear explosion of C/O white dwarfs (WDs), provided the first clear evidence of the Universe’s accelerating expansion (Riess et al. 1998; Perlmutter et al. 1999) and have been used to measure various cosmological parameters (e.g., Hicken et al. 2009; Conley et al. 2011; Sullivan et al. 2011; Suzuki et al. 2012). The two main progenitor scenarios that likely lead to SNe Ia are the single-degenerate (SD) channel, when the WD accretes matter from a nondegenerate companion star (e.g., Whelan & Iben 1973), and the double-degenerate (DD) channel, which is the result of the merger of two WDs (e.g.,

Iben & Tutukov 1984; Webbink 1984).

While it is unclear how often either of these scenarios occur, it seems likely that both are actually present in Nature. For a handful of extremely nearby SNe Ia, many plausible SD scenarios have been ruled out (e.g., Nugent et al. 2011; Foley et al. 2012; Bloom et al. 2012; Silverman et al. 2012b; Schaefer & Pagnotta 2012), and the so-called super-Chandrasekhar mass SNe Ia likely result from the DD scenario (e.g., Howell et al. 2006; Yamamoto et al. 2009; Scalzo et al. 2010; Silverman et al. 2011; Taubenberger et al. 2011). On the other hand, photoionization and subsequent recombination of the circumstellar medium (CSM) created by the progenitor system itself has been observed in a few relatively normal SNe Ia (Patat et al. 2007; Blondin et al. 2009; Simon et al. 2009), and CSM has likely been detected in the spectra of at least 20% of SNe Ia in spiral galaxies (Sternberg et al. 2011). Furthermore, extreme interaction with CSM has been observed in a relatively small number of overluminous SNe Ia mainly via the detection of strong H α emission. These “hybrid” objects also resemble Type II_n SNe (SNe II_n) and have been dubbed SNe Ia-CSM (Silverman et al. 2013b).

Previously, it was not completely clear whether these objects are actually SNe Ia or instead a new subtype of core-collapse SN (e.g., Benetti et al. 2006; Trundle et al. 2008). This controversy seems to have been settled by the discovery and analysis of PTF11kx (Dilday et al. 2012). Discovered on 16 Jan. 2011 (UT dates are used

¹ Department of Astronomy, University of Texas, Austin, TX 78712-0259, USA.

² Department of Astronomy, University of California, Berkeley, CA 94720-3411, USA.

³ email: jsilverman@astro.as.utexas.edu.

⁴ Lawrence Berkeley National Laboratory, Berkeley, CA 94720, USA.

⁵ Benoziyo Center for Astrophysics, The Weizmann Institute of Science, Rehovot 76100, Israel.

⁶ School of Physics and Astronomy, University of Southampton, Southampton, SO17 1BJ, UK.

⁷ Las Cumbres Observatory Global Telescope Network, Goleta, California 93117, USA.

⁸ Department of Physics, University of California, Santa Barbara, CA 93106, USA.

⁹ Department of Physics (Astrophysics), University of Oxford, Keble Road, Oxford OX1 3RH, UK.

¹⁰ INAF, Osservatorio Astronomico di Roma, Via Frascati 33, 00040, Monte Porzio Catone (RM), Italy.

throughout this paper) by the Palomar Transient Factory (PTF; Rau et al. 2009; Law et al. 2009) at redshift $z = 0.0466$ (Dilday et al. 2012) and with Galactic reddening $E(B - V) = 0.052$ mag (Schlegel et al. 1998), it was shown to initially resemble the somewhat overluminous Type Ia SN 1999aa (Li et al. 2001; Strolger et al. 2002; Garavini et al. 2004), though with saturated Ca II H&K absorption lines and weak Na I D lines. This implies the object was almost certainly a SN Ia that had significantly affected its immediate surroundings beginning shortly after explosion.

Subsequent spectra of PTF11kx presented by Dilday et al. (2012) showed time-variable absorption features of Na I, Fe II, Ti II, and He I, which (except for Na I) had not been seen in any previously observed SN Ia. In addition, PTF11kx revealed a strong H α line with a P-Cygni profile (indicative of an expanding shell of material) whose emission component gradually increased in strength, causing the spectra of PTF11kx to eventually resemble those of other Ia-CSM objects (Silverman et al. 2013b). The observations of Dilday et al. (2012) indicate the presence of multiple CSM components with slower-expanding material exterior to faster material and with velocities of ~ 50 – 100 km s $^{-1}$. Recent high-resolution observations of RS Oph (Patat et al. 2011) and models of circumstellar shells created in such systems (Moore & Bildsten 2012) seem to match many of the PTF11kx observations; thus, Dilday et al. (2012) suggest that PTF11kx was a *bona fide* SN Ia with a symbiotic nova progenitor (i.e., a SD scenario, but see Shen et al. 2013). Extending at least some of these findings to *all* of the Ia-CSM objects such that we can say that they are all SNe Ia, likely coming from a SD system, perhaps in the form of a symbiotic nova scenario, is the goal of Silverman et al. (2013b).

In §2 we present eight late-time spectra of PTF11kx, starting with the last spectrum shown by Dilday et al. (2012) from 124 rest-frame days past maximum brightness and continuing through 680 d past maximum. We measure various spectral features and analyze the spectra in §3, and in §4 we compare the spectra of PTF11kx with those of other SNe. We summarize our conclusions in §5.

2. SPECTRA

Figure 1 of Dilday et al. (2012) shows spectra of PTF11kx from 3 d before *B*-band maximum brightness (which was on 29 Jan. 2011) to 88 d past maximum, though one extra spectrum (observed 130 d past maximum, corresponding to 124 d in the rest frame) is listed in their Table S2. This observation is the first one presented in this work, where we extend the spectral coverage of PTF11kx to 680 rest-frame days past maximum brightness.

Low-resolution optical spectra were obtained with the Intermediate dispersion Spectrograph and Imaging System (ISIS)¹¹ on the 4.2 m William Herschel Telescope (WHT), the Low Resolution Imaging Spectrometer (LRIS; Oke et al. 1995) on the Keck-I 10 m telescope, and the DEep Imaging Multi-Object Spectrograph (DEIMOS; Faber et al. 2003) on the Keck-II 10 m tele-

scope. All spectra were reduced using standard techniques (e.g., Silverman et al. 2012a). Routine CCD processing and spectrum extraction were completed with IRAF¹², and flux calibration and removal of telluric lines were done using our own IDL routines. Table 1 lists information regarding the PTF11kx spectra analyzed here, and the data are plotted in Figure 1. Upon publication, all spectra presented in this paper will be available in electronic format on WISeREP (the Weizmann Interactive Supernova data REpository; Yaron & Gal-Yam 2012).¹³

Even though more than 550 rest-frame days are spanned by the data shown in Figure 1, there is not much spectral evolution (until the final spectrum presented). Two of our highest signal-to-noise ratio (S/N) observations are separated by ~ 100 d and are nearly identical (+270 and +371 d). Most of the emission features have disappeared in the latest spectrum shown, from 680 d past maximum brightness. All that is left is the relatively blue “quasi-continuum,” which is likely produced by emission from many overlapping narrow lines of iron-group elements (IGEs, mostly Fe II) excited by the CSM interaction, and H α emission, which has weakened since the previous spectrum (see below for further details). Conspicuously, the Ca II near-infrared (IR) triplet, which is one of the strongest emission features in most of the late-time PTF11kx spectra, is almost completely gone by day +680.

3. ANALYSIS

To better characterize the spectral features seen in PTF11kx, we follow the procedure of Dilday et al. (2012) and fit multiple Gaussian components to the H α and H β emission lines. The H α profiles of our PTF11kx spectra are shown in Figure 2. Clearly the profiles consist of a broader (FWHM ≈ 2000 km s $^{-1}$) component combined with a narrow (FWHM < 200 km s $^{-1}$), unresolved component. While P-Cygni profiles were seen in high-resolution spectra of PTF11kx (Dilday et al. 2012), the spectra presented herein have relatively low resolution, so we do not expect to observe such subtle features.

Figure 3 shows the temporal evolution of the equivalent width (EW; *top*) and flux (*bottom*) of the broader H α component. We find that the broader H α component (after removing the narrow component) is mostly symmetric and slightly blueshifted, perhaps due to the CSM being accelerated somewhat by the SN ejecta. Its EW increases nearly linearly with time until our latest spectrum (from ~ 680 d past maximum brightness), when the EW drops significantly. The H α flux also generally increases with time until a large drop is measured in the last spectrum. Perhaps the decrease in the strength of H α emission at +680 d is indicative of the SN ejecta finally overtaking the majority of the CSM. In their $n = 8$ power-law model of SNe IIn (with $\dot{M}v^{-1} = 5 \times 10^{-4} M_{\odot} \text{ yr}^{-1} \text{ km}^{-1} \text{ s}$), the H α flux is predicted by Chevalier & Fransson (1994) to decrease by a factor of ~ 2 from 1 to 2 yr after maximum brightness. The factor of ~ 4 decrease shown by

¹² IRAF: The Image Reduction and Analysis Facility is distributed by the National Optical Astronomy Observatory, which is operated by the Association of Universities for Research in Astronomy (AURA) under cooperative agreement with the National Science Foundation (NSF).

¹³ <http://www.weizmann.ac.il/astrophysics/wiserep>.

¹¹ <http://www.ing.iac.es/Astronomy/instruments/isis/index.html>

TABLE 1
SPECTRA OF PTF11KX

UT Date	Age (d) ^a	Instrument ^b	Range (Å)	Res. (Å) ^c	Exp. (s)
2011 Jun. 8	124	ISIS	3500–9498	3.5/7.2	3600
2011 Nov. 7	270	ISIS	3500–9500	3.5/7.2	1800
2011 Dec. 26	316	LRIS	5792–7440	3	600
2011 Dec. 26	316	LRIS	3402–10148	3.9/6.1	900
2012 Feb. 21	371	LRIS	3272–10250	3.8/6.0	655
2012 Mar. 15	393	LRIS	3275–5628, 5809–7427	3.6/3	600
2012 Apr. 29	436	LRIS	3236–5630, 5730–7360	3.7/3	625
2013 Jan. 9	680	DEIMOS	4500–9636	3	1800

^aRest-frame days relative to *B*-band maximum brightness (29 Jan. 2011).

^bISIS = Intermediate dispersion Spectrograph and Imaging System on the 4.2 m William Herschel Telescope; LRIS = Low Resolution Imaging Spectrometer on the Keck-I 10 m telescope; DEIMOS = DEep Imaging Multi-Object Spectrograph on the Keck-II 10 m telescope.

^cApproximate resolution, full width at half-maximum intensity (FWHM). If two numbers are listed, they represent the blue-side and red-side resolutions, respectively.

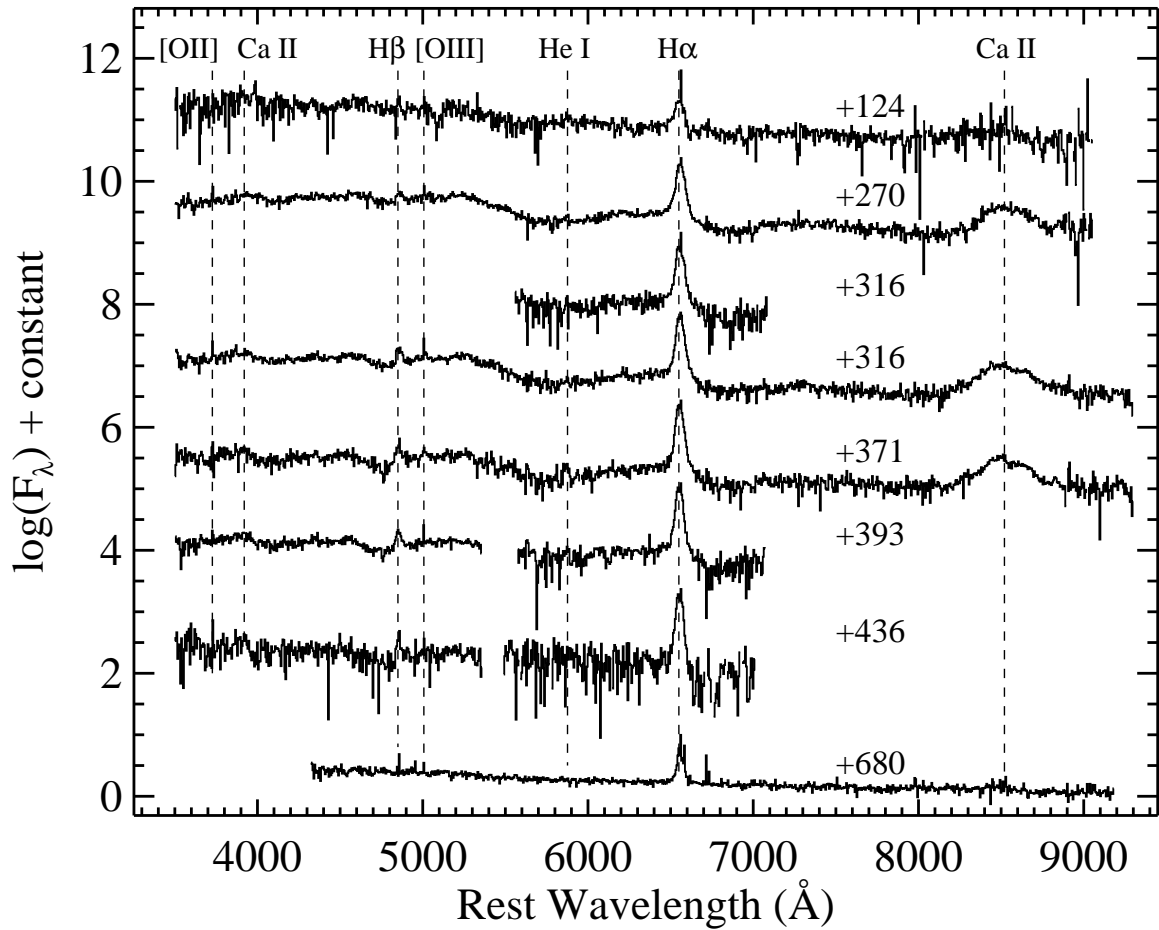


FIG. 1.— Spectra of PTF11kx, labeled with rest-frame age relative to maximum brightness. The locations of detected spectral features, or possible spectral features, are labeled. The data have had their host-galaxy recession velocity removed and have been corrected for Galactic reddening.

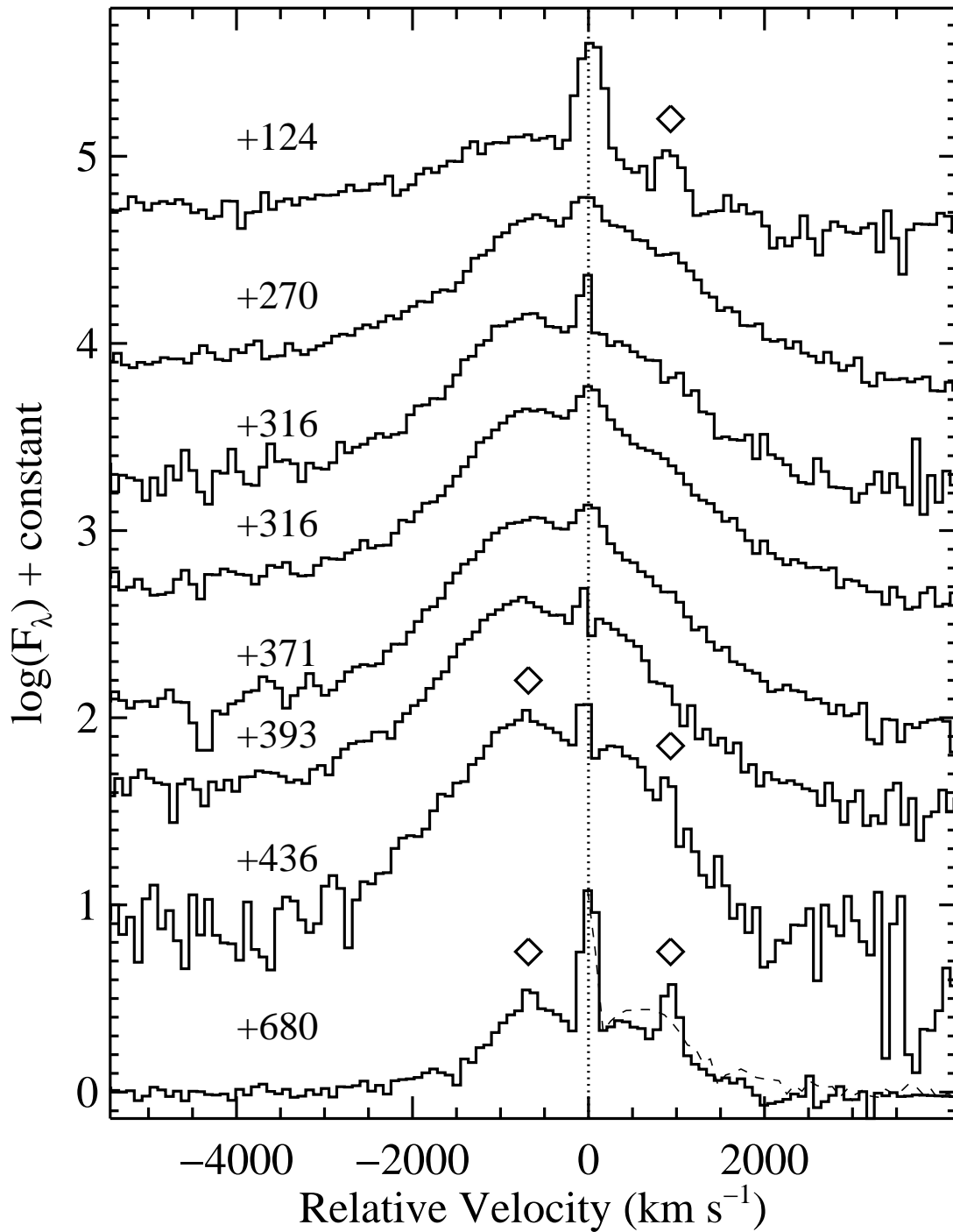


FIG. 2.— The $H\alpha$ profiles of our spectra of PTF11kx, labeled with age relative to maximum brightness. The data have had their host-galaxy recession velocity removed and have been corrected for Galactic reddening. The dotted vertical line is the systemic velocity of PTF11kx. The small emission features marked with diamonds are $[N\ II]\ \lambda 6548.05$ and $\lambda 6583.45$ from the host galaxy. The dashed line on the bottom spectrum is the reflection of the blue half of the $H\alpha$ profile across the peak flux (after removing the $[N\ II]$ emission).

PTF11kx is larger than this prediction, but it occurs at similar epochs. This may indicate that the density structure of the CSM and/or mass-loss history of the PTF11kx system is different than what was nominally assumed by Chevalier & Fransson (1994).

The $H\alpha$ profile in the spectrum from 680 d past maximum exhibits a possible decrease in flux in the red wing as compared to the blue wing. The dashed line on the bottom spectrum in Figure 2 is the reflection of the blue half of the $H\alpha$ profile across the peak flux. This suppression of the red wing has been seen in many SNe IIn and is often interpreted as new dust forming in the post-shock material (e.g., Fox et al. 2011; Smith et al. 2012). This is also observed in all other SNe Ia-CSM, but beginning much earlier (~ 75 – 100 d past maximum brightness; Silverman et al. 2013b).

Narrow emission lines of [O II] $\lambda 3727$, [O III] $\lambda 5007$, and $H\beta$ are apparent in many of the spectra shown in Figure 1. The temporal evolution of the flux of these lines, along with the flux of the narrow component of $H\alpha$ emission, is displayed in the top panel of Figure 4. The flux values have been scaled (by factors of 2, 2.5, and 5 for [O II] $\lambda 3727$, [O III] $\lambda 5007$, and $H\beta$, respectively) in order to emphasize their common evolution. The bottom panel of Figure 4 shows the EWs of these narrow features, again scaled (by factors of 2, 4.5, and 7.5 for [O II] $\lambda 3727$, [O III] $\lambda 5007$, and $H\beta$, respectively) to highlight their common changes with time.

There may be some concern that slit losses, seeing effects, or contamination from nearby H II regions cause the observed variation in these lines with time. However, all observations later than 300 d past maximum brightness were taken under relatively good seeing conditions ($\lesssim 1.1''$) using a $1''$ slit. In addition, the observations from 316 and 371 d past maximum use position angles that differed by $\sim 90^\circ$, and yet they yield nearly *identical* flux (and EW) measurements for all 4 narrow emission lines. On the other hand, the spectra from 371 and 393 d past maximum were obtained using the same position angle, but these data yield significantly *different* flux (and EW) values for each spectral feature. The flux measurements were obtained from the spectra displayed in Figure 1 after scaling each one to nearly contemporaneous photometry of PTF11kx (or a fit to the linear decline of the light curve) shown in Figure 7 below.

The flux and EW of all four emission lines appear in general to decrease, remain constant for ~ 150 d, then perhaps increase again. However $H\alpha$, which is a recombination line and can have a different timescale than the forbidden lines, sometimes behaves significantly differently when compared with the other lines. This could mean that the SN ejecta of PTF11kx are interacting with CSM that is clumpy or perhaps composed of multiple thin shells, which is consistent with what was seen in the early-time spectra (Dilday et al. 2012). It seems unlikely to observe this behavior if the ejecta were expanding into CSM with a monotonically increasing or decreasing density profile, as one might expect from a with a constant mass-loss rate. This conclusion is supported by the extreme late-time overluminosity of PTF11kx (see §4). Nevertheless, we caution that perhaps some of this variability could be caused by slit losses, seeing effects, or contamination from nearby H II regions.

When comparing both the broader and narrower com-

ponents, $H\alpha$ is significantly stronger than $H\beta$ at all epochs. The $H\alpha/H\beta$ intensity ratio is > 7 in all of our late-time spectra of PTF11kx. It varies throughout our observations, but it appears to generally increase with time, peaking at a value of ~ 15 at $t \approx 680$ d. A large, time-variable $H\alpha/H\beta$ intensity ratio seems to be a hallmark of the SN Ia-CSM class (Silverman et al. 2013b).

Another likely tell-tale sign of an object being a SN Ia-CSM is weak He I emission (Silverman et al. 2013b). PTF11kx exhibited weak He I $\lambda 5876$ at early times (Dilday et al. 2012). Figure 5 shows the He I $\lambda 5876$ region in our late-time PTF11kx spectra; we see hints of emission from this feature in some (but not all) cases. The clearest He I $\lambda 5876$ emission is in the form of an unresolved narrow line in our final spectrum at 680 d past maximum brightness. There is no evidence of emission from He I $\lambda 7065$ in any of our spectra, except possibly very weak, unresolved emission again in the 680 d spectrum.

Overplotted (gray dotted line) on the data with the “strongest” resolved He I emission in Figure 5 is the He I $\lambda 5876$ profile at ~ 400 d after discovery of SN 2010jl, a somewhat luminous SN IIn that probably came from a massive star (thus likely *not* a SN Ia of any flavor; Stoll et al. 2011; Smith et al. 2011). The He I $\lambda 5876$ emission is stronger and at higher S/N in SN 2010jl than any of the possible He I $\lambda 5876$ detections in PTF11kx at similar epochs. The most similar feature in the PTF11kx spectra is the possible resolved line on day +371 (see also Fig. 1).

4. COMPARISONS WITH OTHER SUPERNOVAE

In Figure 6 we plot the spectrum of PTF11kx from 316 d past maximum brightness, one of our highest S/N late-time observations. In addition, we show late-time spectra of three other SNe. At these late epochs, PTF11kx resembles the SNe Ia-CSM more than any other SN type. Therefore, we follow the spectral feature identifications that Deng et al. (2004) used for the other prototypical SN Ia-CSM, SN 2002ic (which are also valid for SN 2005gj).

The spectrum of PTF11kx is dominated by relatively narrow $H\alpha$ emission, which is of course also seen in SNe 2005gj and 2010jl (but not in SN 1999aa). The $H\alpha$ emission is somewhat weaker in PTF11kx relative to that of SN 2010jl, but comparable to that of SN 2005gj. Similarly, narrow $H\beta$ emission is detected in PTF11kx, but it is substantially weaker than $H\alpha$ (as mentioned in §3). The strength of the $H\beta$ feature in PTF11kx appears to be intermediate between those of SN 2010jl and SN 2005gj. Higher-order Balmer emission is easily seen in SN 2010jl, but completely undetected in PTF11kx and SN 2005gj.

The broad peak in PTF11kx near 3900 \AA and in PTF11kx and SN 2005gj near 8500 \AA are almost certainly caused in part by Ca II H&K and the Ca II near-IR triplet, respectively, and this latter feature is one of the strongest in both spectra (with FWHM $\sim 10,000 \text{ km s}^{-1}$). Note that emission from these Ca II complexes is also seen in SNe IIn and SNe Ia at late times. In contrast to the +316 d spectrum of PTF11kx shown in Figure 6, there is practically no emission from the Ca II near-IR triplet in the spectrum from 680 d past maximum brightness (see Fig. 1). A model for SNe Ia-CSM that includes a cool dense shell made up of many small fragments containing separate Fe-poor and Fe-rich zones predicts that

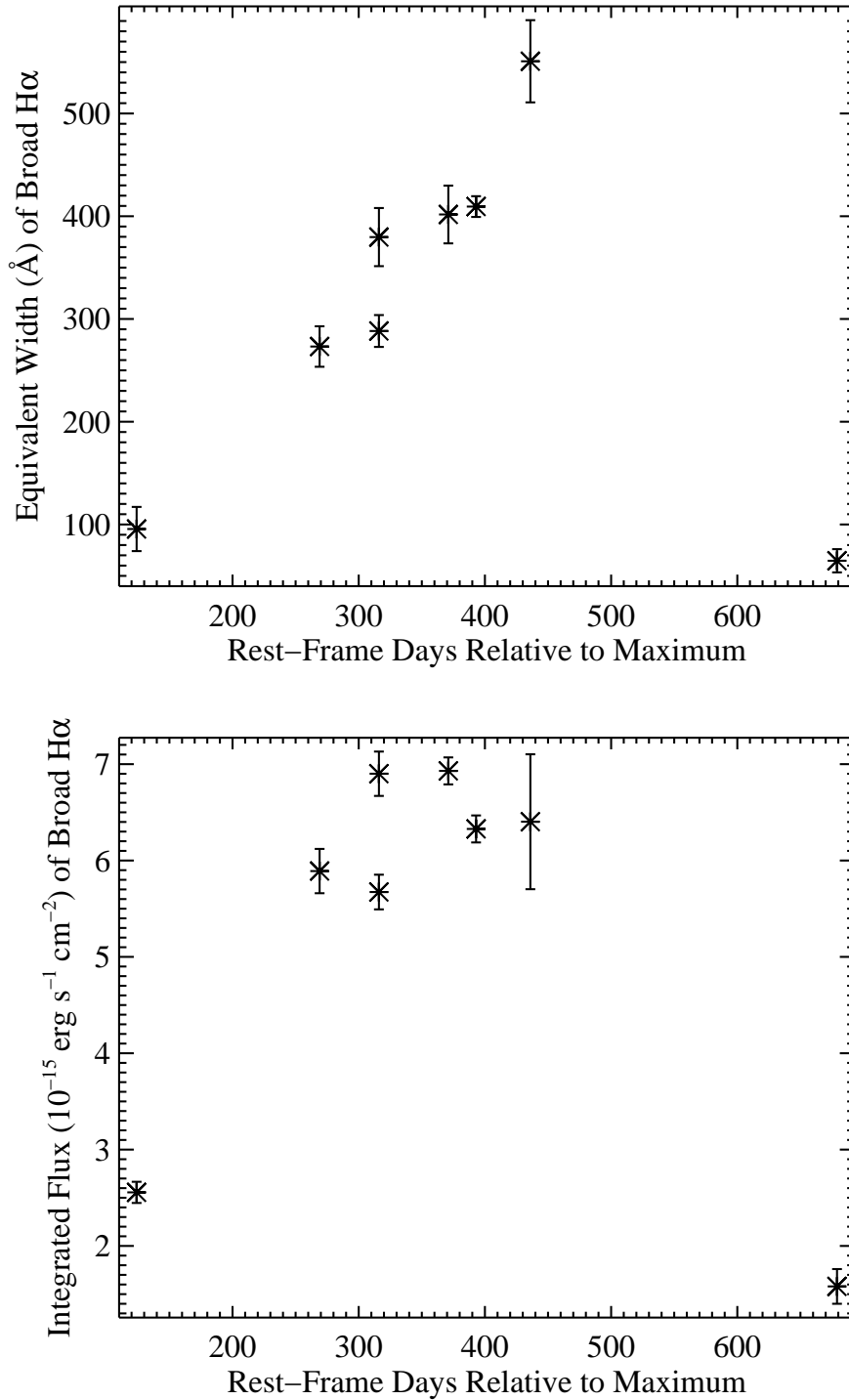


FIG. 3.— Temporal evolution of the EW (*top*) and flux (*bottom*) of the broader H α component.

Ca II emission should disappear once the two zones become fully mixed (Chugai et al. 2004). This was seen to happen in SN 1999E at between 139 and 361 d past maximum (Rigon et al. 2003), and we find the same behavior in PTF11kx but at a later epoch (between 371 and 680 d past maximum).

In all of the spectra shown in Figure 6, the blue flux dramatically increases shortward of ~ 5700 Å. The largest increase in flux at the blue end of the optical range ap-

pears in SN 1999aa, which comes from nebular emission lines from very iron-rich ejecta, excited by radioactivity. On the other hand, the smallest increase in blue flux appears in SN 2010jl, where this blue “quasi-continuum” probably comes from numerous blended, narrow lines of IGEs excited by the CSM interaction. PTF11kx (as mentioned in §2) and SN 2005gj have intermediate amounts of increased blue flux, and since we see evidence of strong CSM interaction in these objects, this “quasi-

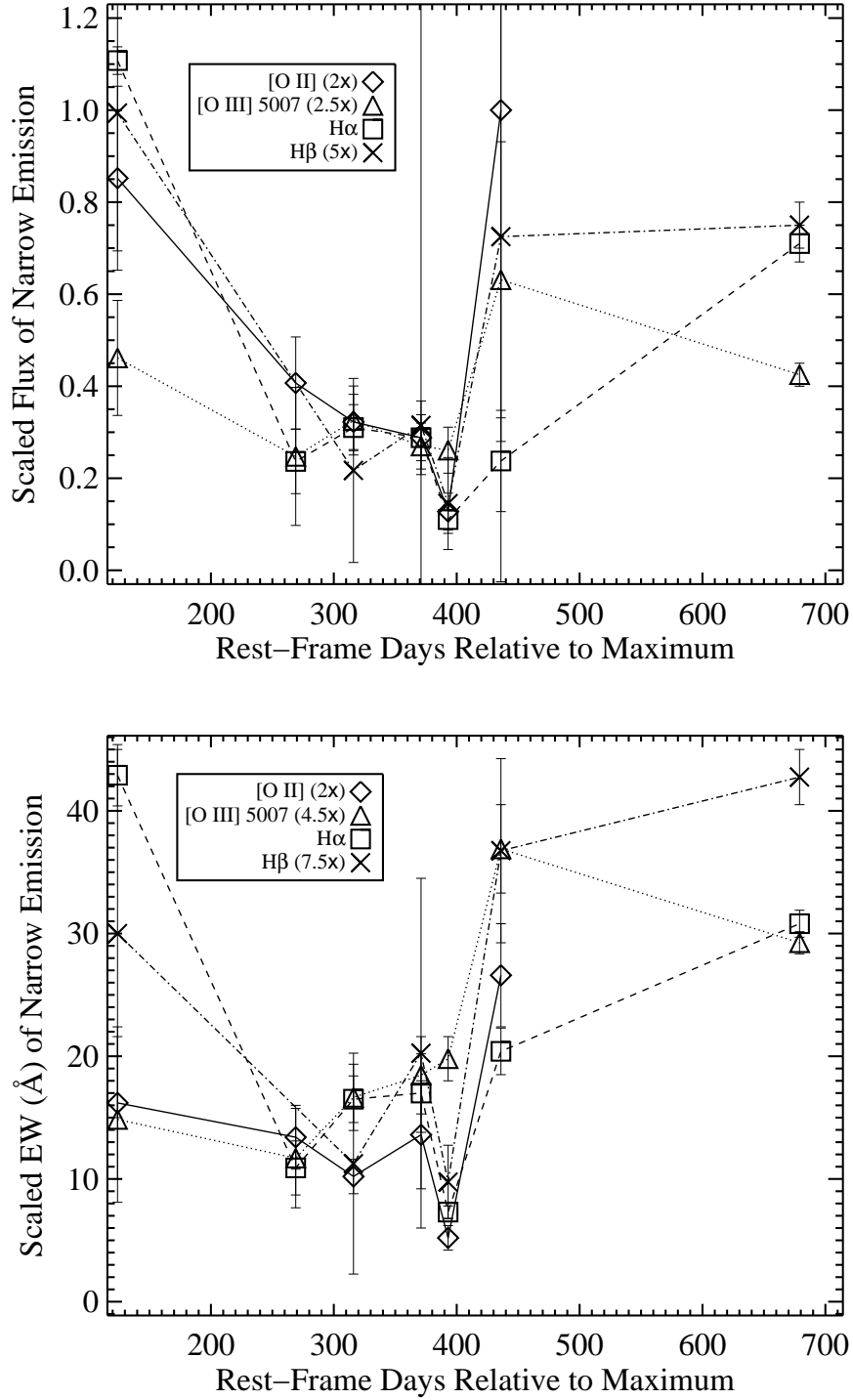


FIG. 4.— The temporal evolution of the flux (*top*) and EW (*bottom*) of the narrow components of [O II] $\lambda 3727$ (diamonds and solid line), [O III] $\lambda 5007$ (triangles and dotted line), H α (squares and dashed line), and H β (Xs and dot-dashed line). The values have been scaled to emphasize their common evolution.

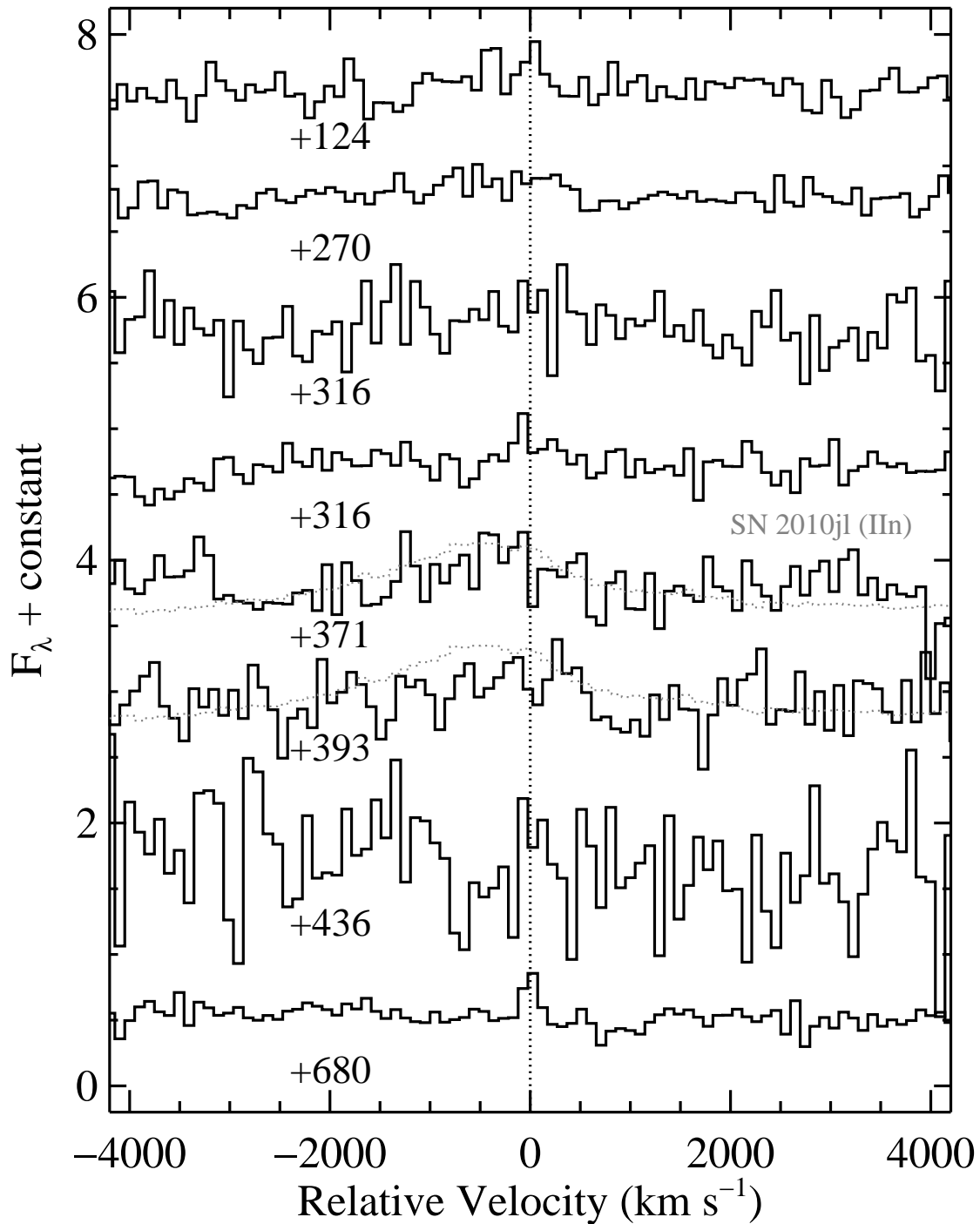


FIG. 5.— The region near He I $\lambda 5876$ in our spectra of PTF11kx, labeled with age relative to maximum brightness. Overplotted (gray dotted line) is the He I $\lambda 5876$ line of SN 2010jl at ~ 400 d after discovery (Smith et al. 2011). The data have had their host-galaxy recession velocity removed and have been corrected for Galactic reddening. The dotted vertical line is the systemic velocity of PTF11kx.

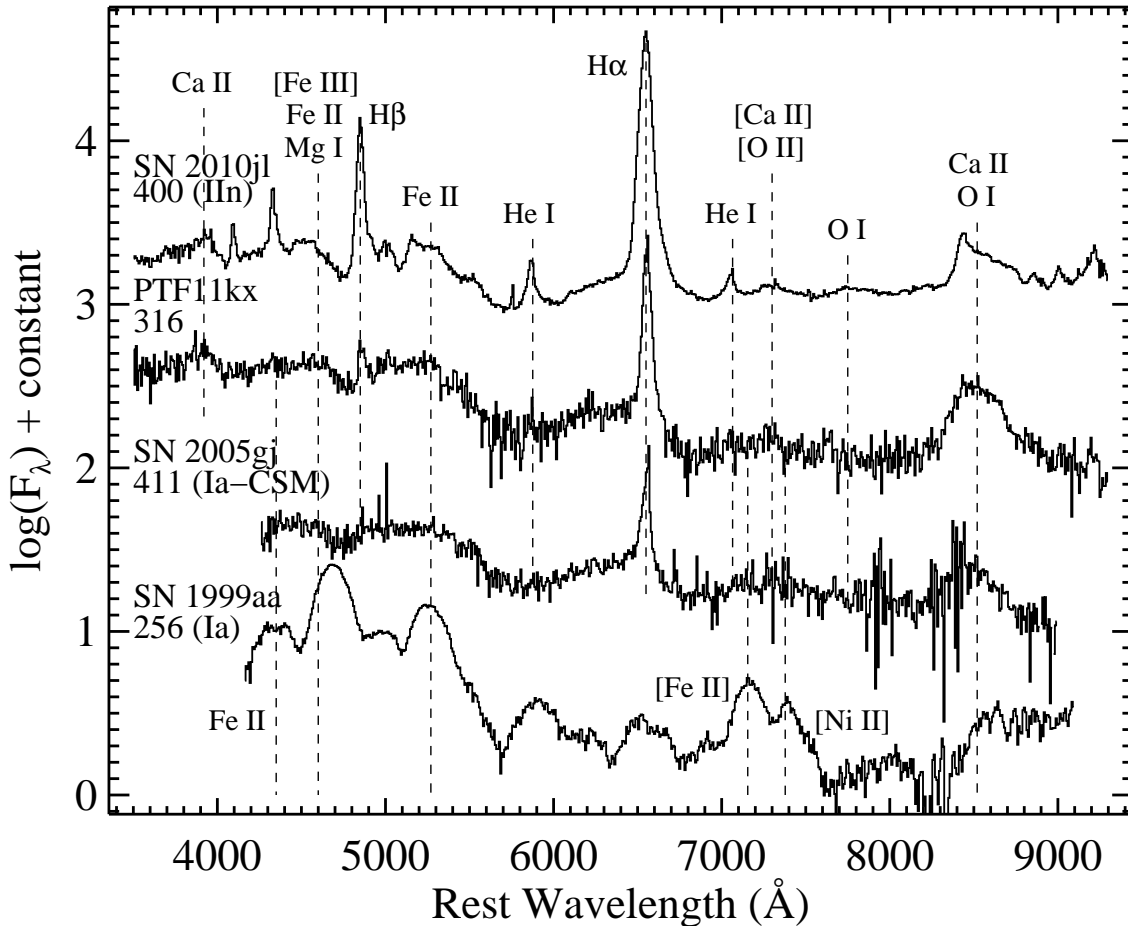


FIG. 6.— The spectrum of PTF11kx from 316 d past maximum brightness, along with three other SNe: the luminous Type IIIn SN 2010jl from ~ 400 d after discovery (Smith et al. 2011); one of the prototypical SNe Ia-CSM, SN 2005gj, from 411 d after maximum brightness (Silverman et al. 2013b); and the somewhat overluminous Type Ia SN 1999aa from 256 d past maximum (Silverman et al. 2012a). Major spectral features are labeled. The data have had their host-galaxy recession velocity removed and have been corrected for Galactic reddening.

continuum” is most likely a stronger version of what is seen in SN 2010jl and less like the nebular emission lines of more normal SNe Ia (such as SN 1999aa, also see below). As most of the optical flux in PTF11kx shortward of ~ 5700 Å comes from numerous IGE multiplets, it is difficult to identify individual features in that wavelength range (aside from Ca II H&K and H β), though some relatively narrow Fe II emission features can be tentatively identified.

The nearly complete lack of emission at ~ 7700 Å in PTF11kx (as well as SN 2005gj) leads us to believe that there is little to no oxygen present in their late-time spectra. Nebular oxygen emission is a hallmark of core-collapse SNe, and it appears in the spectrum of SN 2010jl presented in Figure 6. Thus, this supports the notion that PTF11kx, and all SNe Ia-CSM in general, are in fact genuine SNe Ia. Furthermore, PTF11kx and SN 2005gj exhibit almost no He I (see also §3), while the spectrum of SN 2010jl shows obvious emission lines from He I $\lambda 5876$ and $\lambda 7065$. The almost total lack of oxygen and helium emission in the very late-time PTF11kx spectra imply that the broad, weak emission near 7300 Å is caused either by [Ca II], as it likely is in SN 2010jl, or by [Fe II] and [Ni II], which is what is seen in more typical

SNe Ia at these epochs. We favor the former option since PTF11kx shows no convincing evidence for strong, broad emission features due to [Fe III], [Fe II], or [Ni II] in any of the observations.

These forbidden emission features from IGEs that are typically seen in more normal SNe Ia at late times ($t \gtrsim 100$ d; e.g., Silverman et al. 2013a) may not be detected in PTF11kx since they have been diluted by broad-band continuum flux from the ongoing CSM interaction. Dilday et al. (2012) found that PTF11kx is ~ 16 times more luminous than typical SNe Ia at ~ 100 d past maximum brightness, while more recent observations (shown in Fig. 7) find that it is ~ 300 (~ 2600) times more luminous at ~ 460 d (~ 680 d) past maximum. The extremely slow decline rate at late times [~ 0.2 mag/(100 d)] and the large late-time luminosity of PTF11kx are inconsistent with a CSM model that includes a wind with a constant mass-loss rate (i.e., $\rho \propto r^{-2}$, Chugai & Yungelson 2004). This model was first proposed for SN 2002ic by Chugai & Yungelson (2004), who also showed it to be inconsistent with late-time observations of that object.

At these late epochs, PTF11kx is spectroscopically nearly identical to SN 2005gj (and to the other SNe Ia-CSM as well; e.g., Silverman et al. 2013b). It looks

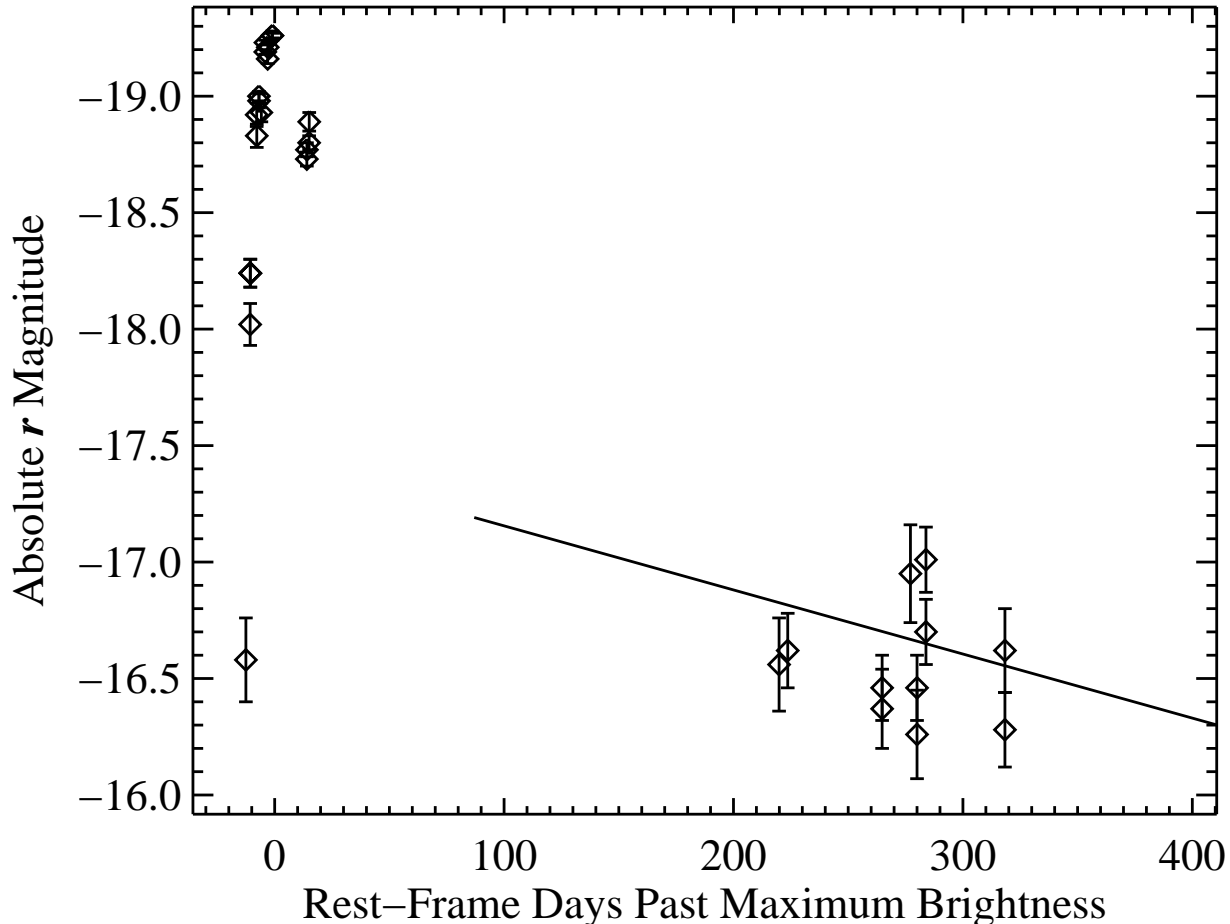


FIG. 7.— The r -band light curve of PTF11kx with data near maximum brightness that come from Dilday et al. (2012). The solid line is the linear late-time decline of ~ 0.2 mag/(100 d).

quite unlike SN 1999aa, even though it closely resembled this object spectroscopically at early times (Dilday et al. 2012). Nebular spectra of other types of SNe Ia were also compared with those of PTF11kx, including the overluminous SN 1991T (Filippenko et al. 1992; Phillips et al. 1992) and the normal SN 2011fe (Bianco et al. in prep.), but as with SN 1999aa, they did not provide good matches. A variety of other SNe IIn were compared to PTF11kx, and in all cases they either closely resembled the spectrum of SN 2010jl presented in Figure 6 or looked completely different from both SN 2010jl and PTF11kx. Finally, we compared PTF11kx to late-time spectra of the normal Type Ic SN 1994I (Filippenko et al. 1995) and the GRB-associated Type Ic SN 1998bw (Patat et al. 2001); we found that while both have a similar amount of blue flux, the spectra of SNe 1994I and 1998bw are dominated by [O I] $\lambda 6300$, [O II] $\lambda 7300$, and Mg I] $\lambda 4571$ emission, which is in stark contrast to the nebular spectra of PTF11kx (and the other SNe Ia-CSM; e.g., Silverman et al. 2013b).

5. CONCLUSIONS

PTF11kx was a SN Ia with high levels of interaction with its CSM, and it likely had a symbiotic nova progenitor (Dilday et al. 2012). In this work we have presented and analyzed late-time spectra of PTF11kx rang-

ing from 124 to 680 d past maximum brightness. While the SN shows very little overall spectral evolution during these epochs (except for the last spectrum), we find that the broader (~ 2000 km s^{-1}) $H\alpha$ emission appears to increase in strength with time for ~ 1 yr, after which time it decreases significantly, perhaps indicating that the SN ejecta have overtaken most of the CSM. There are also indications from the narrow $H\alpha$ component that the ejecta of PTF11kx are interacting with CSM that is clumpy or perhaps made up of multiple thin shells. This is consistent with what was seen in the early-time spectra and the model of a symbiotic nova progenitor which had multiple eruptions prior to the SN (Dilday et al. 2012). We also find that PTF11kx has an unusually large $H\alpha/H\beta$ ratio that varies with time, as well as extremely weak He I emission (significantly weaker than more normal SNe IIn). Both of these are hallmarks of SNe Ia-CSM (Silverman et al. 2013b).

Aside from $H\alpha$, the late-time spectra of PTF11kx also show strong, broad Ca II emission features (FWHM $\sim 10,000$ km s^{-1}). The Ca II emission disappeared nearly completely in the +680 d spectrum, which agrees with a model of another SN Ia-CSM (Chugai et al. 2004). This spectrum also indicates the possibility of newly formed dust in the post-shock material as evidenced by a slight decrease in the red wing of $H\alpha$ compared with the blue

wing. At all epochs little to no emission is detected from oxygen, He I, and Balmer lines (aside from $H\alpha$), which leads to a large observed $H\alpha/H\beta$ intensity ratio in PTF11kx.

When comparing our late-time spectra of PTF11kx with those of other SNe, we have shown that it does not resemble SNe Ic and only bears a passing resemblance to more typical SNe Ia (ones that follow the Phillips 1993 relation). PTF11kx shows a blue “quasi-continuum” (due to numerous blended, relatively narrow lines of Fe II), but broad emission features from [Fe III], [Fe II], and [Ni II] (which are seen in more normal SNe Ia at late times) are absent. These features are completely diluted by the broad-band continuum flux from the ongoing CSM interaction. The extremely slow decline rate at late times, ~ 0.2 mag/(100 d), and the large late-time luminosity, 4–9 mag brighter than a typical SN Ia, are almost certainly caused by the interaction between the SN ejecta of PTF11kx and the CSM.

PTF11kx was a highly special case of a rare type of SN ($\sim 1\%$ of the SN Ia population) being discovered relatively early (~ 7 d after explosion; Dilday et al. 2012). The main observational properties of PTF11kx described above are shared by other SNe Ia-CSM, as well as by more typical SNe IIn. Separating SNe Ia-CSM from SNe IIn and studying the SN Ia-CSM class in greater detail are undertaken by Silverman et al. (2013b). Despite this work and the fortuitous discovery and extensive follow-up observations of PTF11kx, questions still remain. Models of SNe IIn, such as those by Chevalier & Fransson (1994), seem to be somewhat applicable to SNe Ia-CSM, and models of other SNe Ia-CSM (e.g., Chugai et al. 2004; Chugai & Yungelson 2004) appear to match the observations of PTF11kx. These models are a great starting point for future theoretical work that we hope will utilize the observations and analysis presented herein.

We would like to thank J. S. Bloom, K. Clubb, A. A.

Miller, and A. Morgan for their assistance with some of the observations, B. Dilday, O. Fox, and L. Wang for helpful discussions, and the anonymous referee for providing comments and suggestions that improved the manuscript. We are grateful to the staffs at the WHT and the Keck Observatory for their support. The WHT is operated on the island of La Palma by the Isaac Newton Group in the Spanish Observatorio del Roque de los Muchachos of the Instituto de Astrofísica de Canarias. Some of the data presented herein were obtained at the W. M. Keck Observatory, which is operated as a scientific partnership among the California Institute of Technology, the University of California, and the National Aeronautics and Space Administration (NASA); the observatory was made possible by the generous financial support of the W. M. Keck Foundation. The authors wish to recognize and acknowledge the very significant cultural role and reverence that the summit of Mauna Kea has always had within the indigenous Hawaiian community; we are most fortunate to have the opportunity to conduct observations from this mountain. This research has made use of the NASA/IPAC Extragalactic Database (NED) which is operated by the Jet Propulsion Laboratory, California Institute of Technology, under contract with NASA. Funding for SDSS-III has been provided by the Alfred P. Sloan Foundation, the Participating Institutions, the National Science Foundation (NSF), and the U.S. Department of Energy Office of Science. The SDSS-III web site is <http://www.sdss3.org/>. Supernova research by A.V.F.’s group at U.C. Berkeley is supported by Gary and Cynthia Bengier, the Richard and Rhoda Goldman Fund, the Christopher R. Redlich Fund, the TABASGO Foundation, and NSF grants AST-0908886 and AST-1211916. Work by A.G.-Y. and his group is supported by grants from the ISF, BSF, GIF, and Minerva, an FP7/ERC grant, and the Helen and Martin Kimmel Award for Innovative Investigation. M.S. acknowledges support from the Royal Society.

REFERENCES

- Benetti, S., Cappellaro, E., Turatto, M., Taubenberger, S., Harutyunyan, A., & Valenti, S. 2006, *ApJ*, 653, L129
 Blondin, S. et al. 2009, *ApJ*, 693, 207
 Bloom, J. S. et al. 2012, *ApJ*, 744, L17
 Chevalier, R. A. & Fransson, C. 1994, *ApJ*, 420, 268
 Chugai, N. N., Chevalier, R. A., & Lundqvist, P. 2004, *MNRAS*, 355, 627
 Chugai, N. N. & Yungelson, L. R. 2004, *Astronomy Letters*, 30, 65
 Conley, A. et al. 2011, *ApJS*, 192, 1
 Deng, J., Kawabata, K. S., Ohyama, Y., Nomoto, K., Mazzali, P. A., Wang, L., Jeffery, D. J., Iye, M., Tomita, H., & Yoshii, Y. 2004, *ApJ*, 605, L37
 Dilday, B. et al. 2012, *Science*, 337, 942
 Faber, S. M. et al. 2003, in *Proceedings of the Society of Photo-Optical Instrumentation Engineers (SPIE) Conference*, ed. M. Iye & A. F. M. Moorwood, Vol. 4841, 1657
 Filippenko, A. V. et al. 1992, *ApJ*, 384, L15
 —. 1995, *ApJ*, 450, L11
 Foley, R. J. et al. 2012, *ApJ*, 744, 38
 Fox, O. D. et al. 2011, *ApJ*, 741, 7
 Garavini, G. et al. 2004, *AJ*, 128, 387
 Hicken, M., Wood-Vasey, W. M., Blondin, S., Challis, P., Jha, S., Kelly, P. L., Rest, A., & Kirshner, R. P. 2009, *ApJ*, 700, 1097
 Howell, D. A. et al. 2006, *Nature*, 443, 308
 Iben, Jr., I. & Tutukov, A. V. 1984, *ApJS*, 54, 335
 Law, N. M. et al. 2009, *PASP*, 121, 1395
 Li, W., Filippenko, A. V., Treffers, R. R., Riess, A. G., Hu, J., & Qiu, Y. 2001, *ApJ*, 546, 734
 Moore, K. & Bildsten, L. 2012, *ApJ*, 761, 182
 Nugent, P. E. et al. 2011, *Nature*, 480, 344
 Oke, J. B., Cohen, J. G., Carr, M., et al. 1995, *PASP*, 107, 375
 Patat, F., Chugai, N. N., Podsiadlowski, P., Mason, E., Melo, C., & Pasquini, L. 2011, *A&A*, 530, A63
 Patat, F. et al. 2001, *ApJ*, 555, 900
 —. 2007, *Science*, 317, 924
 Perlmutter, S. et al. 1999, *ApJ*, 517, 565
 Phillips, M. M. 1993, *ApJ*, 413, L105
 Phillips, M. M., Wells, L. A., Suntzeff, N. B., Hamuy, M., Leibundgut, B., Kirshner, R. P., & Foltz, C. B. 1992, *AJ*, 103, 1632
 Rau, A. et al. 2009, *PASP*, 121, 1334
 Riess, A. G. et al. 1998, *AJ*, 116, 1009
 Rigon, L. et al. 2003, *MNRAS*, 340, 191
 Scalzo, R. A. et al. 2010, *ApJ*, 713, 1073
 Schaefer, B. E. & Pagnotta, A. 2012, *Nature*, 481, 164
 Schlegel, D. J., Finkbeiner, D. P., & Davis, M. 1998, *ApJ*, 500, 525
 Shen, K. J., Guillochon, J., & Foley, R. J. 2013, *ApJ*, accepted (arXiv:1302.2916)
 Silverman, J. M., Ganeshalingam, M., & Filippenko, A. V. 2013a, *MNRAS*, 529
 Silverman, J. M., et al. 2013b, *ApJS*, in press
 Silverman, J. M., Ganeshalingam, M., Li, W., Filippenko, A. V., Miller, A. A., & Poznanski, D. 2011, *MNRAS*, 410, 585
 Silverman, J. M. et al. 2012a, *MNRAS*, 425, 1789
 —. 2012b, *ApJ*, 756, L7
 Simon, J. D. et al. 2009, *ApJ*, 702, 1157

- Smith, N., Silverman, J. M., Filippenko, A. V., Cooper, M. C., Matheson, T., Bian, F., Weiner, B. J., & Comerford, J. M. 2012, *AJ*, 143, 17
- Smith, N. et al. 2011, *ApJ*, 732, 63
- Sternberg, A. et al. 2011, *Science*, 333, 856
- Stoll, R. et al. 2011, *ApJ*, 730, 34
- Strolger, L. et al. 2002, *AJ*, 124, 2905
- Sullivan, M. et al. 2011, *ApJ*, 737, 102
- Suzuki, N. et al. 2012, *ApJ*, 746, 85
- Taubenberger, S. et al. 2011, *MNRAS*, 412, 2735
- Trundle, C., Kotak, R., Vink, J. S., & Meikle, W. P. S. 2008, *A&A*, 483, L47
- Webbink, R. F. 1984, *ApJ*, 277, 355
- Whelan, J. & Iben, Jr., I. 1973, *ApJ*, 186, 1007
- Yamanaka, M. et al. 2009, *ApJ*, 707, L118
- Yaron, O. & Gal-Yam, A. 2012, *PASP*, 124, 668